ACOUSTIC BAND GAP MATERIALS

J.H. Page[1], A.L. Goertzen[1,*], Suxia Yang[1,2], Zhengyou Liu[2,3], C.T. Chan[2] and Ping Sheng[2]

[1] Department of Physics and Astronomy, University of Manitoba, Winnipeg MB Canada R3T 2N2
[2] Department of Physics, Hong Kong University of Science and Technology, Clear Water Bay, Kowloon, Hong Kong, China
[3] Department of Physics, South China University of Technology, Guangzhou 510640 China

INTRODUCTION

In recent years, there has been a growing interest in the propagation of acoustic and elastic waves in periodic composite materials. Such materials are the acoustic or elastic analogue of photonic crystals, and in both cases, much of the interest has focussed on theoretical and experimental studies of spectral gaps due to the periodicity of the underlying structure [1-11]. For sound, these are often referred to as phononic band gaps, by analogy with photonic band gaps for light and electronic band gaps for metals. Motivation for studying materials with phononic band gaps is driven in part from potential applications, examples being their role in sound filters, transducer design and acoustic mirrors. Of possibly greater interest from the fundamental scientific perspective is the rich physics of acoustic and elastic systems, where scattering contrast is affected by both density and velocity differences, and the waves can have mixed longitudinal and transverse vector character, leading to the possibility of novel propagation phenomena. These features of phononic band gap materials may also make them interesting candidates for studies of wave localization.

Although the theory of acoustic and elastic band gap materials is now quite well developed, there have been relatively few experimental studies of these materials [7-11]. Most of these experiments have focussed on two-dimensional structures, where the experimental realization of a complete spectral gap has been demonstrated. In this paper, we turn to three dimensional materials, and present recent pulsed ultrasonic transmission measurements on hexagonal close packed (hcp) arrays of monodisperse stainless steel beads immersed in water. We use this system to illustrate how ultrasonic techniques provide a powerful experimental tool for studying classical wave propagation in periodic composite media, some of the advantages of these techniques including the ability to

measure the wave field directly, and the relative ease with which pulsed techniques can be used over a wide range of frequencies. By measuring the ultrasonic wave field transmitted through slab-shaped samples of different thicknesses, we determine both the dispersion curve and amplitude transmission coefficient. Because the field is pulsed, we can also measure the group velocity and investigate the dynamics of the wave fields [12] in phononic crystals. We interpret our experimental results by comparing them with theoretical calculations based on a multiple scattering theory (MST) for acoustic and elastic waves [5, 6], which is ideally suited to the spherical scatterer geometry of the present experiments. We show that this theoretical approach gives a good description of the low-frequency band structure and transmission coefficient measured in our experiments.

EXPERIMENT

The phononic crystals used in our experiments were constructed from monodisperse spherical steel beads surrounded by a continuous matrix of water. This choice of materials provides high scattering contrast in our ultrasonic experiments, because of the large difference in both density and velocity of the two constituent media (for the steel beads, the longitudinal and shear velocities are v_L = 6.01 km/s and v_S = 3.23 km/s, and the density is ρ = 7.67×10^3 kg/m^3, while for water v_L = 1.49 km/s and ρ = 1.0×10^3 kg/m^3). The steel bead diameter was 0.8014 ± 0.0006 mm, so that the variation in diameter from bead to bead was less than 0.15%, with the deviation from spherical shape of an individual bead being even less at 0.08%. The beads were assembled into a hexagonal close packed (hcp) array by placing the beads very carefully by hand in an acrylite cell. To ensure a defect-free crystal, the cell consisted of a flat bottom plate with hexagonal side walls, which were accurately positioned to constrain the bottom layer of beads into a close-packed triangular lattice. This template allowed subsequent layers to be added in an ABABAB… sequence of triangular arrays to form an hcp lattice with *c*-axis perpendicular to the layers. Although painstaking to carry out, this procedure allowed very high quality crystals to be assembled, thanks to the excellent monodispersity of the beads. Two crystals in the shape of hexagonal slabs were assembled, each with dimensions in the *ab* plane much greater than along the *c*-axis, so that edge effects at the side walls could be neglected. The thickness of the two crystals was 3.41 and 6.69 mm, corresponding to 5 and 10 layers respectively.

To measure the ultrasonic field transmitted though the phononic crystals, the samples were placed horizontally in a water tank, which provided a convenient coupling medium between the ultrasonic transducers and the sample cell. We used a pulsed technique, in which planar immersion broadband transducers were placed on each side of the sample; the transducers were oriented so that the pulsed ultrasonic beam traveled upwards from the generating transducer through the sample to the receiving transducer, as shown by the schematic diagram in Fig. 1. This orientation allowed the beads to be held in place by gravity, avoiding the need for a top wall, which would have complicated the boundary conditions on the sample cell. The bottom supporting wall was made sufficiently thick that no multiple reflections in the wall could arrive at the bottom face of the sample until after the initial transmitted pulse through the sample had decayed to below the detection noise threshold. A small-diameter transducer was used to generate the pulses, and the distance between the transducer and sample was chosen to be large enough so that the sample was well into the far field of the transducer, where the input pulse was an excellent approximation to a plane wave over the cross section of the sample. The detecting transducer had a larger diameter (25 mm) allowing it to selectively measure the spatially and temporally coherent component of the field transmitted along the c-axis of the crystal.

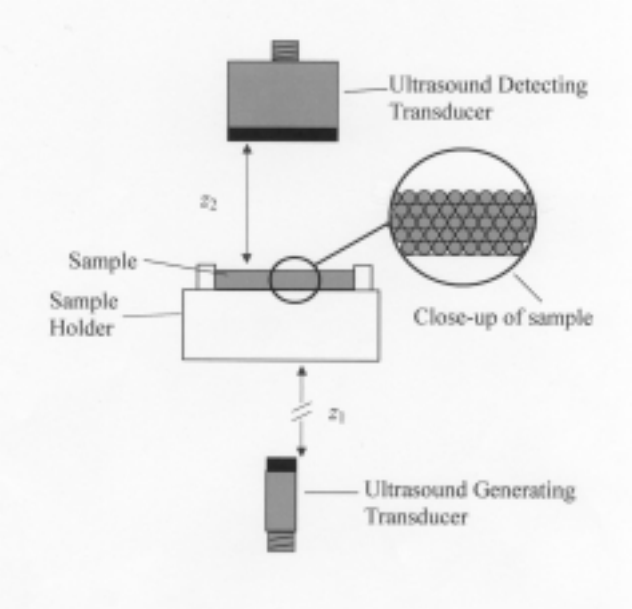

FIGURE 1: Schematic diagram of the experimental setup.

The transmitted field detected by the top transducer was amplified with a low-noise high-gain receiving amplifier, signal averaged using a digital oscilloscope, and then downloaded to a computer for subsequent analysis. To permit the effects of the support wall at the bottom of the cell to be taken into account, the transmitted field was first measured without the sample and support wall in place, then through the support wall only, and finally through the crystal sample placed on top of its supporting wall.

Our pulse propagation experiments allow us to measure the phase velocity, the group velocity and the attenuation of the ultrasonic waves as a function of frequency, thus fully characterizing wave transport through the phononic crystal and enabling the bandstructure and amplitude transmission coefficient to be measured. In the left column of Fig. 2, we compare a typical short input pulse that is incident at the support wall/sample interface with the corresponding pulses that are transmitted through the 5-layer and 10-layer samples. One advantage of using a short input pulse is that it allows the transmitted field to be measured over a wide frequency range, determined by the bandwidth of the transducers (typically $\pm$ 50% of the central frequency) in a single measurement. Short input pulses also allow the interference effects due to Bragg scattering in the crystal to be observed in real time, as indicated by the considerable broadening and modulation of the pulses transmitted through the samples that is shown in the two lower figures in the left column of Fig. 2. However, because of this pulse distortion, the velocities at which the waves travel though the crystal cannot be determined directly in the time-domain from such short pulses. Instead, we digitally filter the transmitted waveforms using a narrow-band Gaussian filter centered at frequency $f = \omega / 2\pi$, using a sufficiently narrow filter bandwidth that the filtered pulses extend over a range of times long enough to incorporate the contributions to the net phase from all multiply reflected waves in the sample. To determine the frequency dependence of the velocities, the process is repeated over the entire frequency range spanned by the transducers. Two examples of such digitally filtered pulses are shown in the middle and right columns of Fig. 2, for central frequencies of 0.5 MHz and 1.0 MHz respectively. In both cases, the bandwidth was 0.01 MHz, sufficiently narrow to give excellent Gaussian pulses for both the input and transmitted, waves with minimal distortion

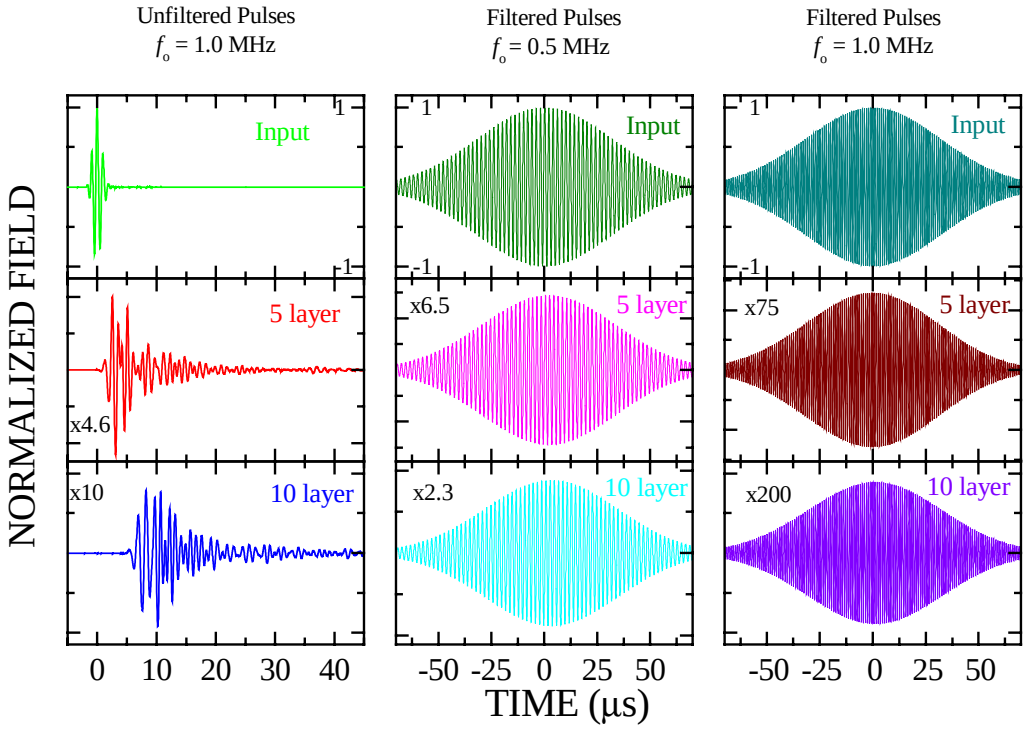

FIGURE 2: Input and transmitted pulses through the 5 and 10 layer samples (left) compared with digitally filtered pulses at a bandwidth of 0.01 MHz (middle and right columns).

and broadening due to dispersive effects. For these digitally filtered pulses, the phase delay between the filtered input and transmitted pulses is well defined, allowing the phase velocity v_p to be determined, at the central frequency of the pulse, from the ratio of the sample thickness to the measured phase delay. The measurements were performed down to low enough frequencies that uncertainties in the phase shift of multiples of 2π could be unambiguously eliminated, as there was then only one possible value that gave physically realistic velocities. The correct value of the phase delay was also confirmed by the consistency of the measurements made at the two sample thicknesses. Note that this method of determining the phase delay is equivalent to measuring the phase difference directly from the fast Fourier transforms of the input and transmitted pulses [13]. However, one advantage of our digital filtering method is that it also allows the group velocity to be measured directly from the pulse propagation time. By visual inspection of Fig. 2, it is clear that the group velocity is faster at 1.0 MHz than it is at 0.5 MHz. To measure the group velocity quantitatively, we determine the envelopes of the transmitted pulses, and measure the group velocity from the ratio of the sample thickness to the time interval between the peaks of the pulses, the latter being obtained accurately using a least squares fitting routine. The filtered pulses in Fig. 2 also give information of the amplitude transmission coefficient, which is given at the central frequency of the pulses by the ratio of the peak heights of the transmitted and input pulses. In practice, it is simpler to measure the frequency dependence of the amplitude transmission coefficient directly from the ratio of the fast Fourier transforms of the unfiltered transmitted and input pulses, thus obtaining the frequency dependence over the entire bandwidth of the transducers in one step.

THEORY

We have recently developed a multiple scattering theory (MST) for elastic waves that is ideally suited to calculating the band-structure of phononic crystals containing solid spherical scatterers embedded in a fluid matrix [6]. A similar model for acoustic waves has also been formulated recently by Kafesaki and Economou [5]. For this type of phononic material, the more common plane wave method has been shown to be unable to give accurate results [5]. By contrast, the MST, which is based on the same approach as the Korringa-Kohn-Roskoker (KKR) theory for electronic band-structure calculations, exhibits advantages in handling specialized geometries such as the spherical scatters in the present work. In the MST for elastic waves, the band-structure is determined by calculating the elastic Mie scattering of the waves incident on a single scatter from all the other scatterers in the crystal, and solving the resulting secular equation for the eigenfrequencies. Details of the calculation are given elsewhere [6]. Here we show the predictions of the MST for the phononic band-structure of our steel bead/water hcp crystal in Fig. 3. For this high contrast hcp crystal, the lowest gap in the spectrum is large along the *c*-axis, although it shrinks and becomes very narrow between the M and K points, so that there is only a very small complete phononic band gap in this material.

We have also extended the multiple scattering theory to describe the reflection and transmission of elastic waves by finite slabs of periodically arranged scatterers [6]. These reflection and transmission calculations are based on a double-layer scheme, in which the reflection and transmission matrix elements for a multilayer slab are obtained from those of a single layer. The advantage of this approach is that it allows direct comparison of theory with experiments on finite systems, where it is important to account for the effects of the boundary conditions. Examples of the predictions of this theory are given in the next section where the experimental results are discussed.

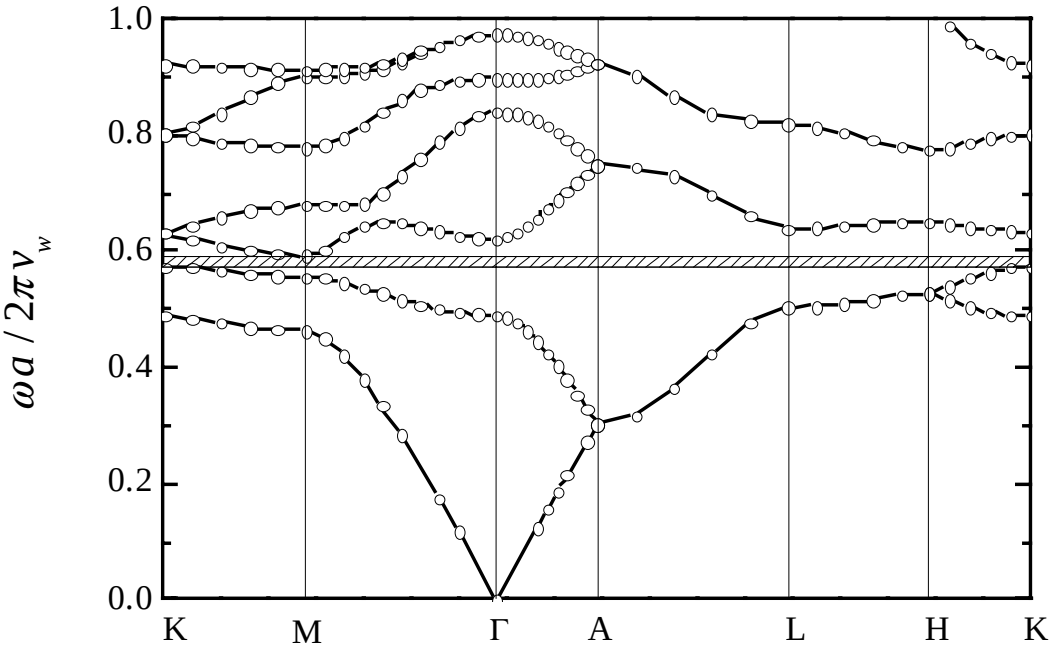

FIGURE 3: Band structure of an hcp crystal of stainless steel spheres in water. Here *a* is the lattice constant in the basal plane and v_w is the sound velocity in water.

RESULTS AND DISCUSSION

Using the experimental and theoretical techniques described in the previous two sections, we have investigated the ultrasonic transmission, pulse propagation and band-structure along the *c*-axis of our hcp steel/water crystals. In figure 4, we plot the amplitude transmission coefficient as a function of frequency for both the 5 and 10-layer samples, with the experimental results in the upper panels and the theory in the lower ones. The deep minima in the transmission indicate the frequencies at which gaps occur in dispersion curve along the *c*-axis, these minima becoming wider and deeper as the sample thickness is increased and the spectral gaps become better defined. Considering the finite thickness of the crystals, the depth of some of the minima is remarkably large, with the transmitted intensity dropping by 2 to 6 orders of magnitude depending on the gap location. Note that the frequencies at which these minima occur in the upper panels are in very good agreement with those in the lower panels of Fig. 4, indicating excellent correspondence between the multiple scattering theory and experiment. In addition to the large maxima and minima, there are smaller regular oscillations in the transmitted amplitude that become more closely spaced as the sample thickness increases. This behaviour is consistent with the interference of multiple reflections from the top and bottom surfaces of the crystal, as was confirmed by calculating the positions of the oscillation peaks using measured data for the phase velocity in the sample. Figure 4 shows that theoretical calculations give a good description of the overall structure of the measured transmission coefficient, although the theoretical predictions are consistently higher in magnitude. This difference becomes greater at higher frequencies and may be attributed to ultrasonic absorption in the sample, an effect that has not been included in the present calculations.

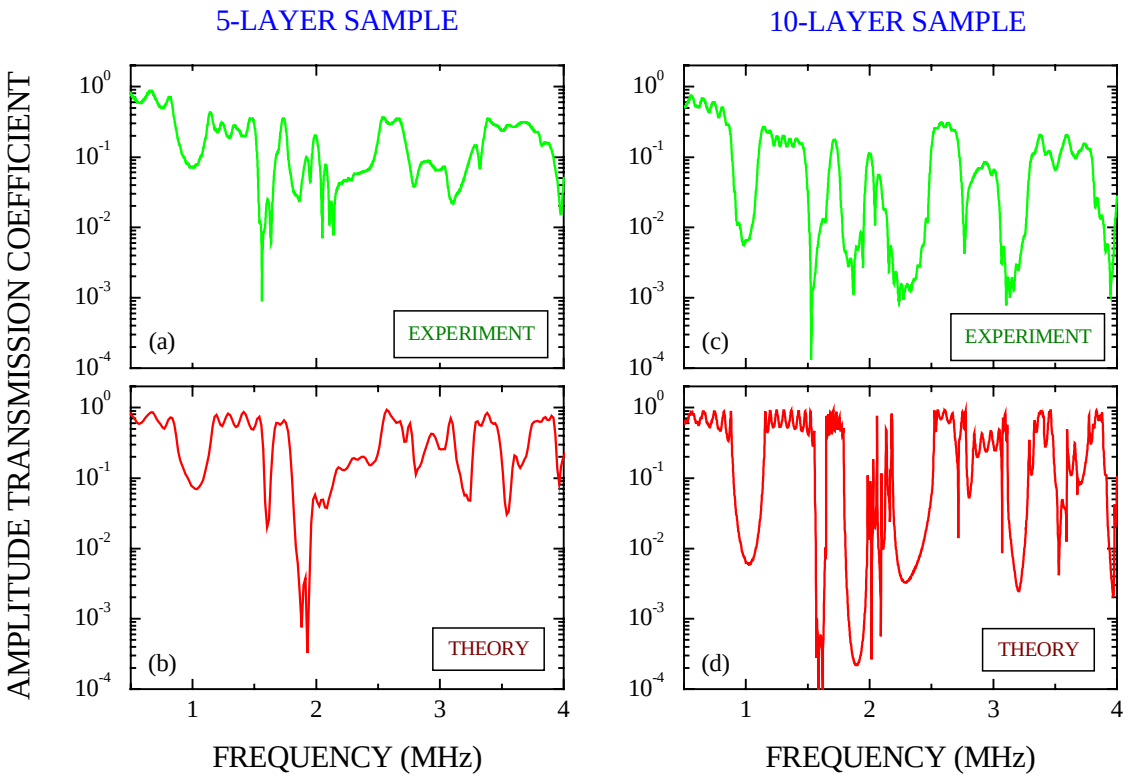

FIGURE 4: Frequency dependence of the amplitude transmission coefficient for the 5 and 10 layer samples (left and right panels respectively).

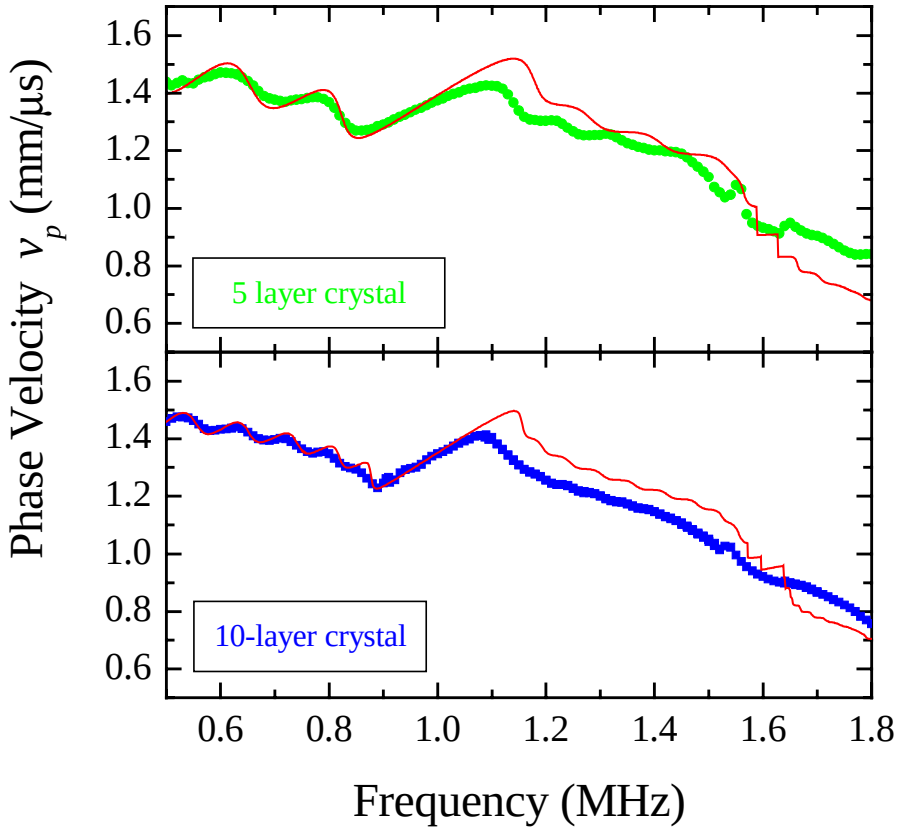

FIGURE 5: Frequency dependence of the phase velocity. The symbols and curves represent experiment and theory respectively.

The frequency dependence of the phase velocity is plotted in Fig. 5, where we focus on the behavior for frequencies below 2 MHz, the range over which the phase velocity changes most significantly. The experimental results (solid symbols) are compared with the theoretical predictions of the MST (solid curves), determined from the phase of the complex transmission coefficient. At the lowest frequencies, the phase velocity is close to the value for pure water but drops off markedly as the frequency increases, eventually reaching values less than half the phase velocity in water as the higher frequency energy bands flatten out. There is also considerable structure in the frequency dependence of v_p over this range. The same interference effect (due to boundary reflections) that modulates the transmission also causes the net phase to oscillate, leading to periodic variations in the phase velocity that are especially pronounced (and more widely spaced) for the thinner sample. Since the spacing of the oscillations is $\Delta f = v_p/2L$, their presence can be used to confirm that the cumulative phase, from which the phase velocity is determined, has been correctly unwrapped. Note the generally excellent agreement between theory and experiment for the positions of the oscillations, the one exception being the results for the 5-layer sample above 1.2 MHz, where there is an offset. Also, the magnitude of the oscillations is less in the experimental data, another manifestation of the absorption present in the sample. Of greater interest is the variation in the phase velocity associated with the band gaps. In the lowest gap centered at 1MHz the velocity increases with frequency as expected, although the experimental data show a narrower gap than the theory. Perhaps more surprising is the fact that neither the theory or experiment for v_p show a very pronounced increase at the second gap between 1.5 and 1.6 MHz, despite quite sharp drops

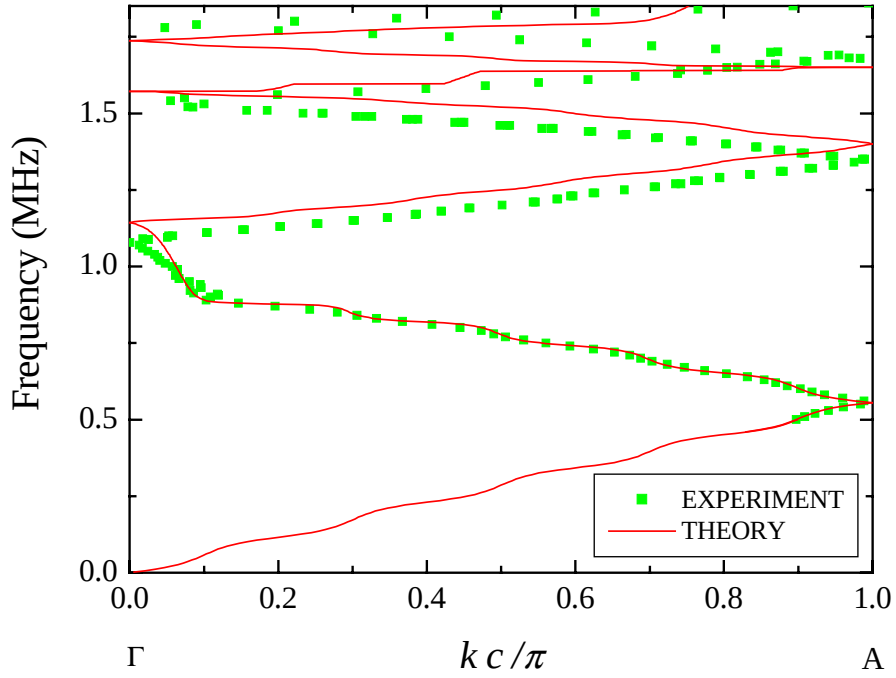

FIGURE 6: Comparison of the measured dispersion curve parallel to the c direction (symbols) with the predictions of the MST theory for the transmission (curves).

in the transmission (Fig. 4), as well as a clear gap in the infinite-crystal band structure (c.f. Fig. 3), in this frequency range.

These measurements of the phase velocity can also be used to determine the dispersion curve parallel to the *c* direction, either directly in the extended zone scheme, or in the more commonly used reduced zone scheme. The reduced zone scheme dispersion curve for the 10-layer sample is shown in Fig. 6; it was obtained in the usual way by subtracting multiples of the reciprocal lattice vector $G_{001} = 2\pi/c$ from k and making use of the symmetry of the dispersion curve about $\pm k$. In Fig. 6, our experimental results (solid symbols) are compared with the theoretical predictions of the MST theory for the transmission (solid curves). As for the plot of the phase velocity, the overall agreement between theory and experiment is very good over this range of frequencies. However, at higher frequencies the agreement is worse, possibly due to small imperfections in the crystal that have a greater effect at shorter wavelengths.

To gain a more complete picture of wave propagation through phononic crystals, we investigate the frequency dependence of the group velocity. We are not aware of any previous measurements of the group velocity in phononic crystals, although there have been several reports of optical pulse propagation in both 1D and 3D photonic crystals [12, 14-16]. Our results in the frequency range between 0.5 and 1.5 MHz are shown in Fig. 7, where again we compare experiment with MST theory, using solid symbols and curves respectively, for the two sample thicknesses. We find a very large variation in v_g over this frequency range, with the experimental data varying by about one order of magnitude, and even larger structure being exhibited in the theory, obtained by differentiating the MST dispersion curve. As with the transmission coefficient and the phase velocity, the larger variation seen in the theory can be attributed to the effects of absorption, which cuts off the long multiple scattering paths. Note the marked decrease (by about a factor of 3 relative to the values near 0.5 MHz) in the group velocity as the band gap at 1 MHz is approached

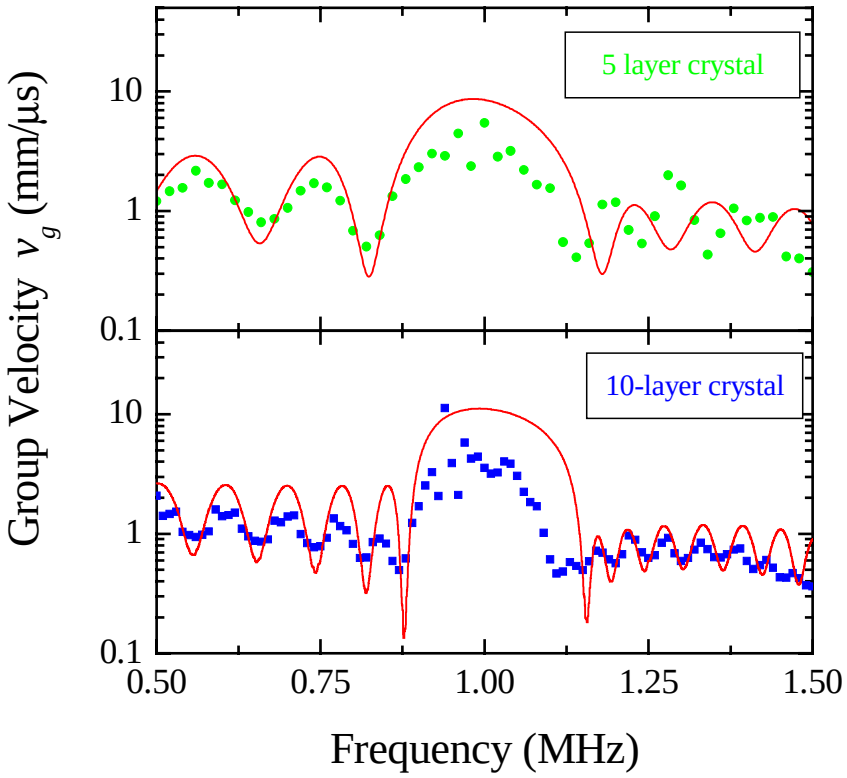

FIGURE 7: Frequency dependence of the group velocity. The symbols and curves represent experiment and theory respectively.

from either side, with even smaller values of v_g, comparable to the velocity of sound in air, being reached in the fourth pass band at the upper end of the frequency range shown. Inside the lowest band gap, there is considerable scatter in the experimental data, as the transit time becomes quite short compared with the pulse width; none-the-less, a significant increase in v_g is seen, rising to values between those of pure water and steel. By analogy with previous optical measurements in 1D photonic crystals [14, 15], we ascribe the mechanism underlying these large values of v_g to be ultrasonic pulse tunneling through the gap. These measurements thus give a direct measure of the tunneling time, the first time that this has been measured for ultrasonic waves in a phononic crystal.

CONCLUSIONS

We have presented experimental and theoretical results for ultrasonic wave propagation in a hcp phononic crystal made from stainless steel beads immersed in water. Our pulsed experiments measure the frequency dependence of the phase and group velocities, as well as the attenuation of the ultrasonic waves, giving new information on the band structure and transmission in this phononic crystal. Our data are interpreted using a multiple scattering theory, which gives good overall agreement with the experiments, especially at low frequencies where the absorption is less pronounced. We are currently working on extending the MST for elastic waves to include the effects of absorption, by including viscous losses at the interfaces between the water and the solid spheres.

ACKNOWLEDGEMENTS:

Support from NSERC of Canada and RGC of Hong Kong is gratefully acknowledged.

REFERENCES

* Present address: Crump Institute for Biological Imaging, Department of Molecular and Medical Pharmacology, UCLA School of Medicine, Los Angeles, CA 90095-1770, USA

[1] E. N. Economou and M. Sigalas, J. Acoust. Soc. Am. **95**, 1734 (1994).

[2] A. D. Klironomos and E. N. Economou, Solid State Comm **105**, 327 (.1998).

[3] M. S. Kushwaha, P. Halevi, and G. Martinez, Phys. Rev. B **49**, 2313 (1994).

[4] M. Sigalas and E. N. Economou, Europhys. Lett. **36**, 241 (1996).

[5] M. Kafesaki and E. N. Economou, Phys. Rev. B **60**, 11993 (1999).

[6] Z. Liu, C. T. Chan, P. Sheng, A. L. Goertzen, and J. H. Page, Phys. Rev. B, in press (2000).

[7] J. V. Sanchez-Peres, *et al*., Phys. Rev. Lett. **80**, 5325 (1998).

[8] F. R. Montero de Espinosa, E. Jimenez, and M. Torres, Phys. Rev. Lett. **80**, 1208 (1998).

[9] J. O. Vasseur, P. A. Deymier, G. Frantziskonis, G. Hong, B. Dijafari-Rouhani, and L. Dobrzynski, J.Phys.: Condens. Matter **10**, 6051 (1998).

[10] D. Caballero, J. Sanchez-Dehesa, C. Rubio, R. Martinez-Sala, J. V. Sanchez-Perez, F. Meseguer, and J. Llinares, Phys. Rev. E **60**, R6316 (1999).

[11] R. E. Vines and J. P. Wolfe, Physica B **263-264**, 567 (1999).

[12] A. Imhof, W. L. Vos, R. Sprik, and A. Lagendijk, Phys. Rev. Lett. **83**, 2942 (1999).

[13] W. M. Robertson, G. Arjavalingam, R. D. Meade, K. D. Brommer, A. M. Ragge, and J. D. Joannopoulos, Phys. Rev. Lett. **68**, 2023 (1992).

[14] A. M. Steinberg, P. G. Kwist, and R. Y. Chiao, Phys. Rev. Lett. **71**, 708 (1993).

[15] C. Spielmann, R. Szipocs, A. Stingl, and F. Krausz, Phys. Rev. Lett. **73**, 2308 (1994).

[16] M. Scalora, *et al*., Phys. Rev. E **54**, R1078 (1996).